Supplemental Figure 1. Intravital imaging of hair follicles over an entire hair cycle, remodeling of dermal papilla fibroblasts, and consequences of fibroblast ablation, related to Figure 1-2

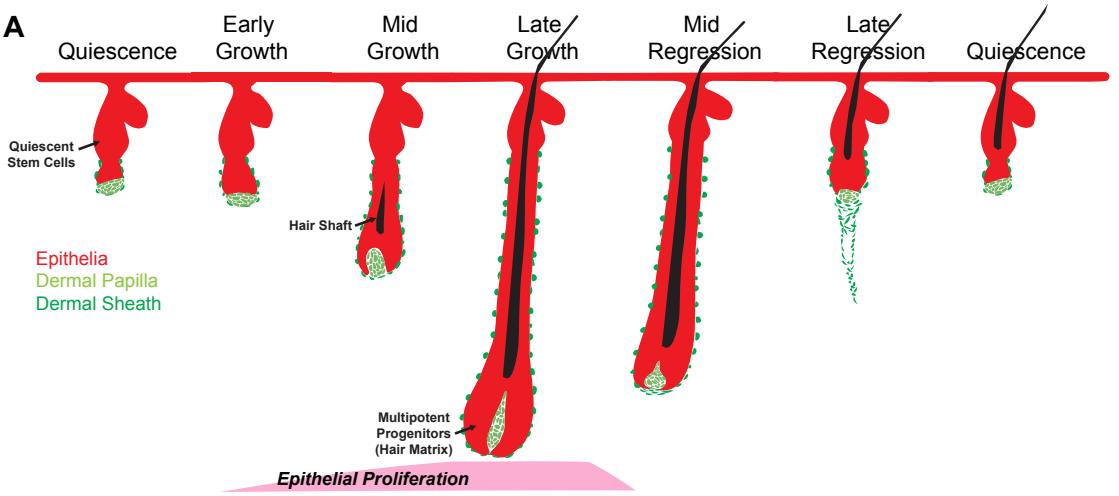

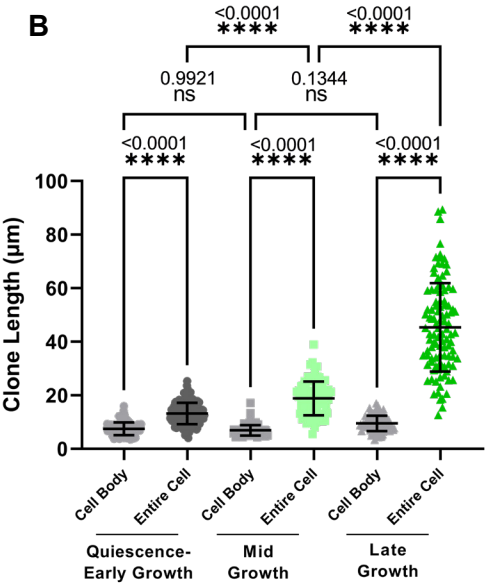

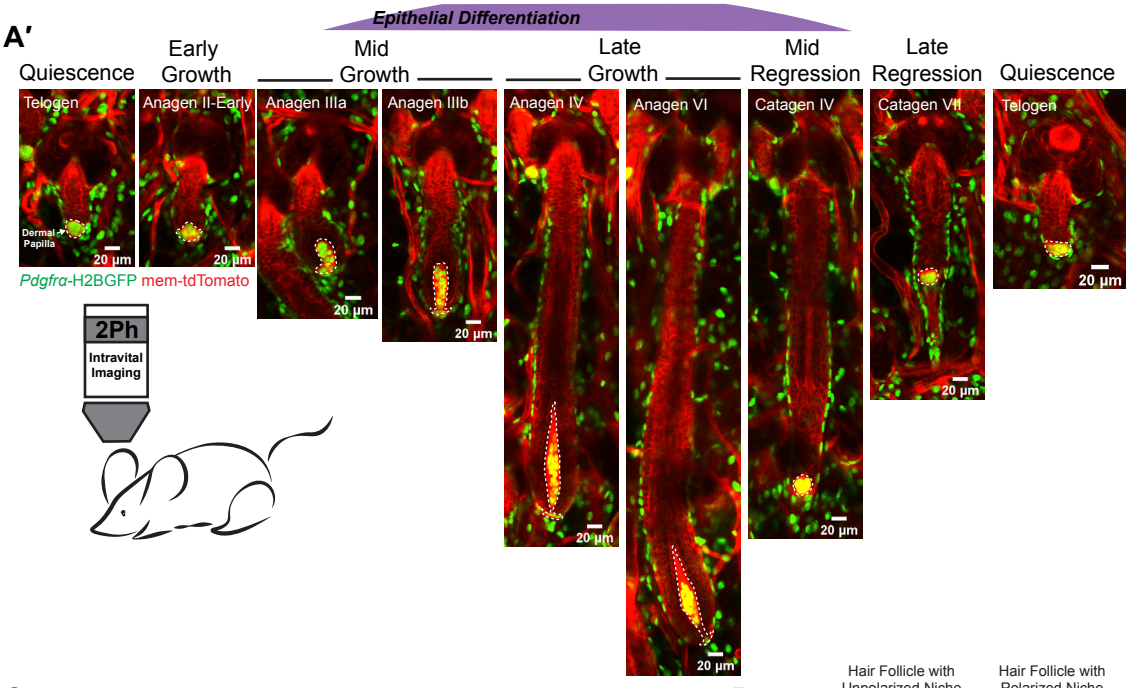

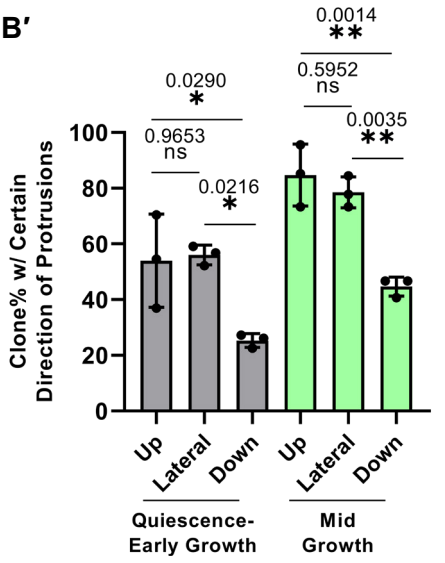

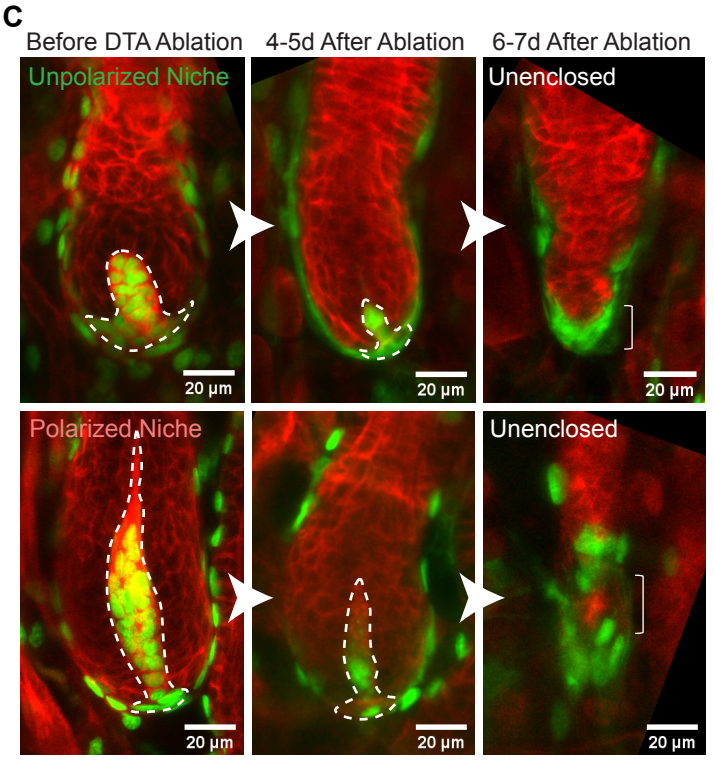

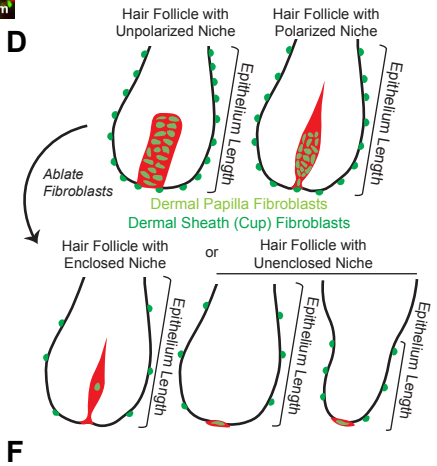

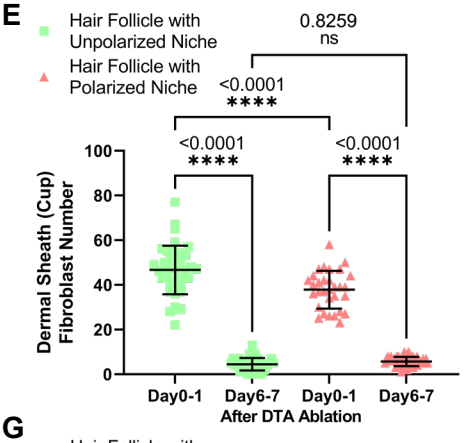

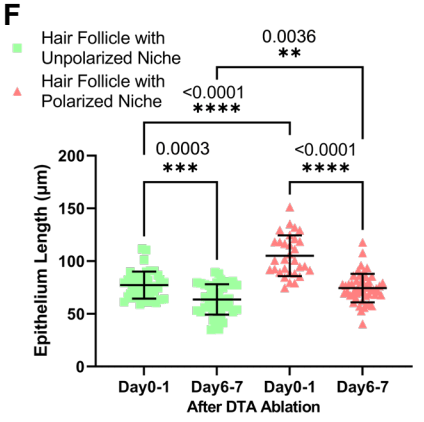

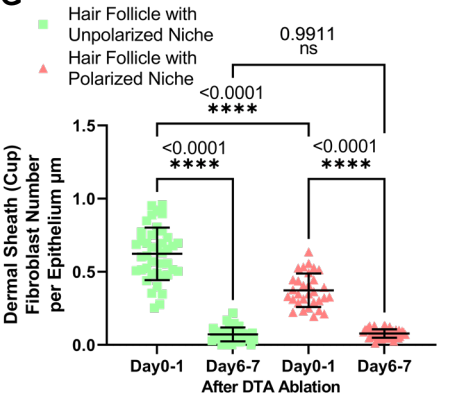

SUPPLEMENTAL FIGURES AND LEGENDS

Supplemental Figure 1. Intravital imaging of hair follicles over an entire hair cycle, remodeling of dermal papilla fibroblasts, and consequences of fibroblast ablation, related to Figure 1-2

A. Schematic of the remodeling hair follicle epithelium (red) and associated fibroblasts, including dermal sheath (dark green) and dermal papilla (light green). Time windows of epithelial proliferation and differentiation are indicated in pink and purple.

A′. Intravital images of hair follicles at different stages. *Pdgfrα*-H2BGFP labels all fibroblast nuclei in green and membrane-tdTomato labels all cell membranes in red. The dermal papillae are white dash-lined at the bottom of hair follicles. As the hair follicle grows, the dermal papilla becomes enclosed, elongated, and returns to a compact ball architecture during regression. All representative images are single optical z slice with scale bar sizes indicated.

B. Length of dermal papilla fibroblast cell bodies and entire cell membranes at different hair cycle stages. Data are presented as mean ± S.D. n=160 dermal papilla fibroblast clones at quiescence-early growth from 3 mice. n=88 dermal papilla fibroblast clones at mid-growth from 3 mice. n=103 dermal papilla fibroblast clones at late-growth from 3 mice. Tukey's multiple comparisons test.

B′. Percentage of dermal papilla fibroblasts harboring certain direction of membrane protrusions (upward, lateral, downward) at quiescence-early growth and mid-growth. Data are presented as mean ± S.D. n=161 dermal papilla fibroblast clones at quiescence-early growth from 3 mice. n=87 dermal papilla fibroblast clones at mid-growth from 3 mice. Tukey's multiple comparisons test.

C. Longitudinally imaged dermal papillae that become unenclosed after diphtheria toxin (DTA)-induced fibroblast ablation (*Pdgfrα*-CreER; LSL-DTA). Fibroblast nuclei are labeled in green by *Pdgfrα*-H2BGFP, and cell membranes are in red by membrane-tdTomato. Before DTA ablation and 4-5 days after ablation, dash-lined dermal papillae are enclosed within the epithelium; some of these become unenclosed and locate at the bottom of hair follicle epithelium 6-7 days after ablation (bracketed). Representative images are summed optical z slices with scale bar sizes indicated.

D. Schematic illustrating the consequences of *Pdgfrα*-CreER driven DTA ablation in fibroblasts around the hair follicles with unpolarized or polarized niches. After fibroblast ablation, hair follicles' dermal papillae either remained enclosed or became unenclosed. Changes of dermal sheath (cup) fibroblast number (Fig.S1E) and density (Fig.S1G) were quantified based on the bracketed epithelial regions where dermal sheath (cup) fibroblasts normally occupy at the hair follicle bottom.

E. Number of dermal sheath (cup) fibroblasts 0-1 day and 6-7 day after ablation in hair follicles with unpolarized niche or polarized niche. Fibroblast number is counted based on green fibroblast nuclear signal labeled by *Pdgfrα*-H2BGFP. Data are presented as mean ± S.D. For hair follicles with unpolarized dermal papillae at mid-growth, n=41 (Day0-1) and 42 (Day6-7) from 3 mice; for hair follicles with polarized dermal papillae at late-growth, n=31 (Day0-1) and 50 (Day6-7) from 3 mice. Tukey's multiple comparisons test.

F. Length of epithelial regions (bracketed in Fig.S1D) 0-1 day and 6-7 day after ablation in hair follicles with unpolarized niche or polarized niche. Data are presented as mean ± S.D. For hair follicles with unpolarized dermal papillae at mid-growth, n=41 (Day0-1) and 42 (Day6-7) from 3 mice; for hair follicles with polarized dermal papillae at late-growth, n=31 (Day0-1) and 50 (Day6-7) from 3 mice. Tukey's multiple comparisons test.

G. Density of dermal sheath (cup) fibroblasts 0-1 day and 6-7 day after ablation in hair follicles with unpolarized niche or polarized niche. Fibroblast density was calculated as the total number of dermal sheath (cup) fibroblast (Fig.S1E) divided by the epithelium length (Fig.S1F). Data are presented as mean ± S.D. For hair follicles with unpolarized dermal papillae at mid-growth, n=41 (Day0-1) and 42 (Day6-7) from 3 mice; for hair follicles with polarized dermal papillae at late-growth, n=31 (Day0-1) and 50 (Day6-7) from 3 mice. Tukey's multiple comparisons test.

Supplemental Figure 2. Smad4 reporter mouse generation, short- and long-term niche architecture changes in *Tgfbr1*$^{fl/fl}$ hair follicles, and TGFβ signaling activity changes in *Tgfbr1*$^{fl/fl}$ hair follicles, related to Figure 3-4

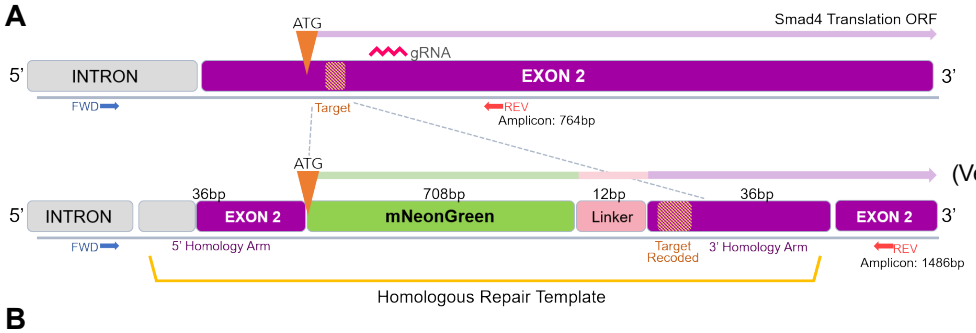

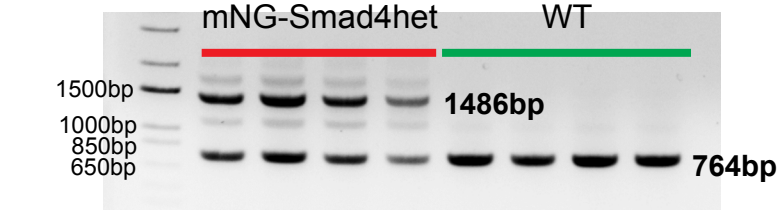

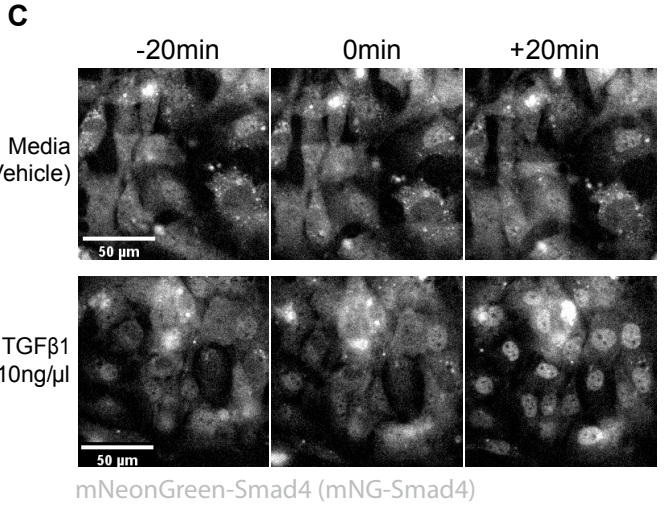

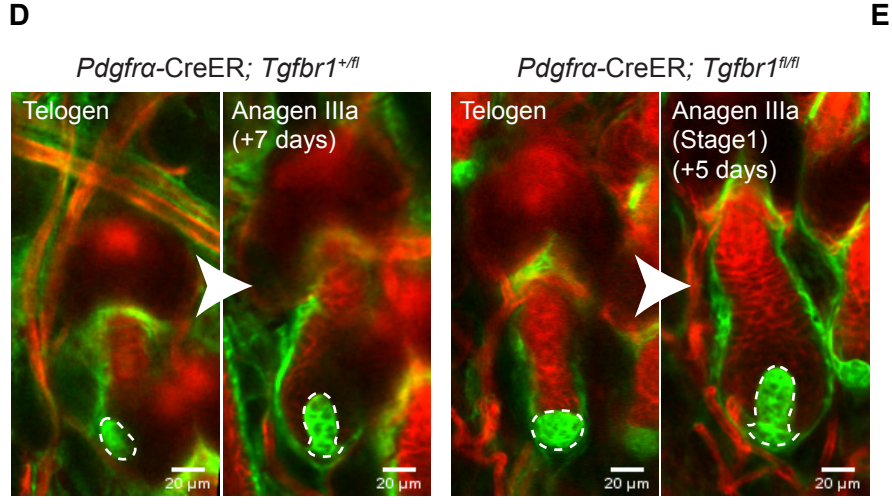

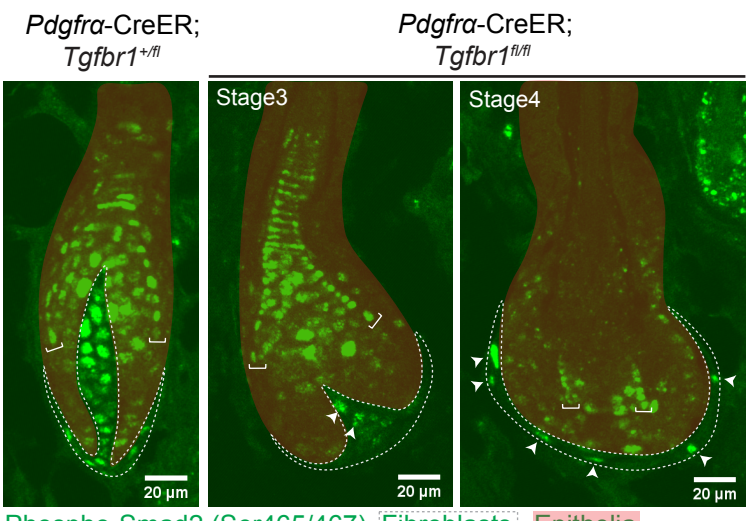

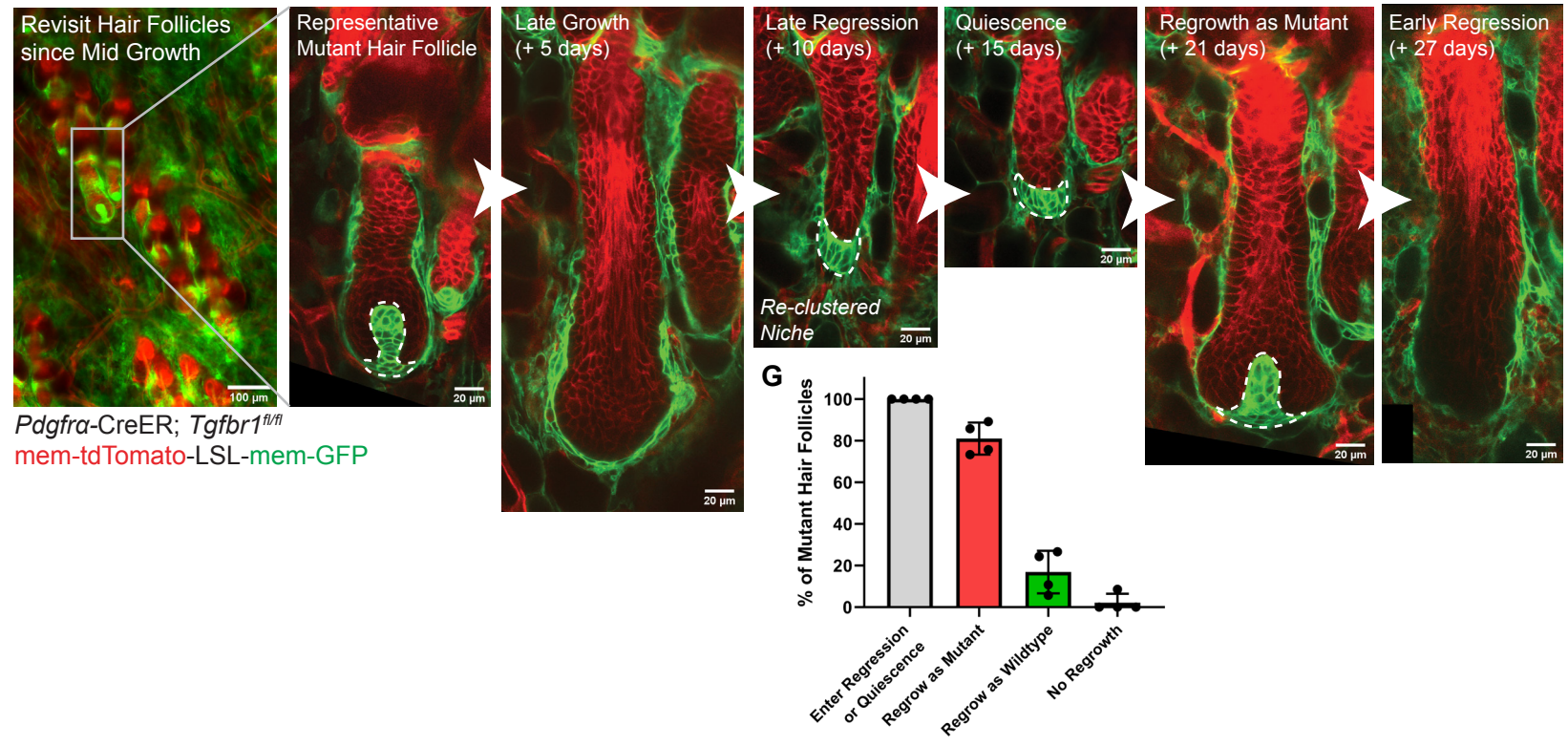

Supplemental Figure 2. Smad4 reporter mouse generation, short- and long-term niche architecture changes in *Tgfbr1*$^{fl/fl}$ hair follicles, and TGFβ signaling activity changes in *Tgfbr1*$^{fl/fl}$ hair follicles, related to Figure 3-4

A. Schematic of the endogenous Smad4 locus in wild-type (above) and mNeonGreen-Smad4 mouse (below) following CRISPR-Cas9-guided homology-directed repair. mNeonGreen (mNG) and a 12bp linker sequence were inserted immediately upstream of the Smad4 start codon in exon 2, flanked by 36bp homology arms. Codons in the CRISPR gRNA target and PAM sequence were replaced with silent mutations to prevent further recombination. Red and blue arrows indicate the positions of genotyping PCR oligos and expected amplicon size.
B. Representative gel electrophoresis image showing genotyping PCR of mNG-Smad4. In addition to the wild-type 764bp amplicon (green), heterozygous mNG-Smad4 mice have an additional 1486bp band (red) indicating the integrated repair template.
C. Representative still images of mouse embryonic fibroblasts derived from mNG-Smad4 heterozygote mice. 20 minutes into imaging, live cells were stimulated with TGF-β1 (10ng/μl) or vehicle. Images were acquired every 5 min and are shown here at 20 min intervals; scale bar sizes indicated. Nuclear localization of mNG-Smad4 remained stable for approximately 7 hours following stimulation.
D. Revisits at quiescence (Telogen) and mid-growth (Anagen IIIa) of the same *Tgfbr1*$^{+/fl}$ or *Tgfbr1*$^{fl/fl}$ dermal papillae, after *Pdgfrα*-CreER induction in quiescence. The dermal papillae remained enclosed within the epithelium until mid-growth. Fibroblast membranes are labeled in green membrane-GFP and other membranes are in red membrane-tdTomato. Dermal papillae are dash-lined. Representative images are single optical z slice with scale bar sizes indicated.
E. Immunostaining for phospho-Smad2 (Ser465/467) (green) in thick back skin sections to detect the presence and distribution of nuclear phospho-Smad2 in the hair follicle epithelium (red masked) and associated dermal papilla and derma sheath fibroblasts (dash-lined). Despite the overall reduction of nuclear phospho-Smad2 staining in *Tgfbr1*$^{fl/fl}$ hair follicles, a few fibroblasts with nuclear phospho-Smad2 signal remained (arrowheads). In addition, the nuclear phospho-Smad2-positive differentiating epithelial progenitors also retained their concentric organization (bracketed). Representative images are single optical z slice with scale bar sizes indicated. n=3 *Tgfbr1*$^{+/fl}$ and 3 *Tgfbr1*$^{fl/fl}$ mice.
F. Long-term revisits of the same *Tgfbr1*$^{fl/fl}$ dermal papilla over weeks from the mid-growth stage (Anagen IIIa) to the next hair cycle. Fibroblast membranes are labeled in green membrane-GFP and other membranes are in red membrane-tdTomato. The lower magnification image on the left is summed optical z slices and other images are single optical z slice with scale bar sizes indicated. Clustered dermal papillae (-like structure) are dash-lined.
G. Percentage of *Tgfbr1*$^{fl/fl}$ mutant hair follicles that enter regression or quiescence phase, regrow as mutant, as wild-type, or fail to regrow in the next hair cycle. n=4 *Tgfbr1*$^{fl/fl}$ mice (145 revisited hair follicles quantified for regression/quiescence entry, 139 revisited hair follicles quantified for regrowth). Data are presented as mean ± S.D.

Supplemental Figure 3. Characterization of molecular changes in *Tgfbr1*$^{fl/fl}$ mutant fibroblasts, related to Figure 3

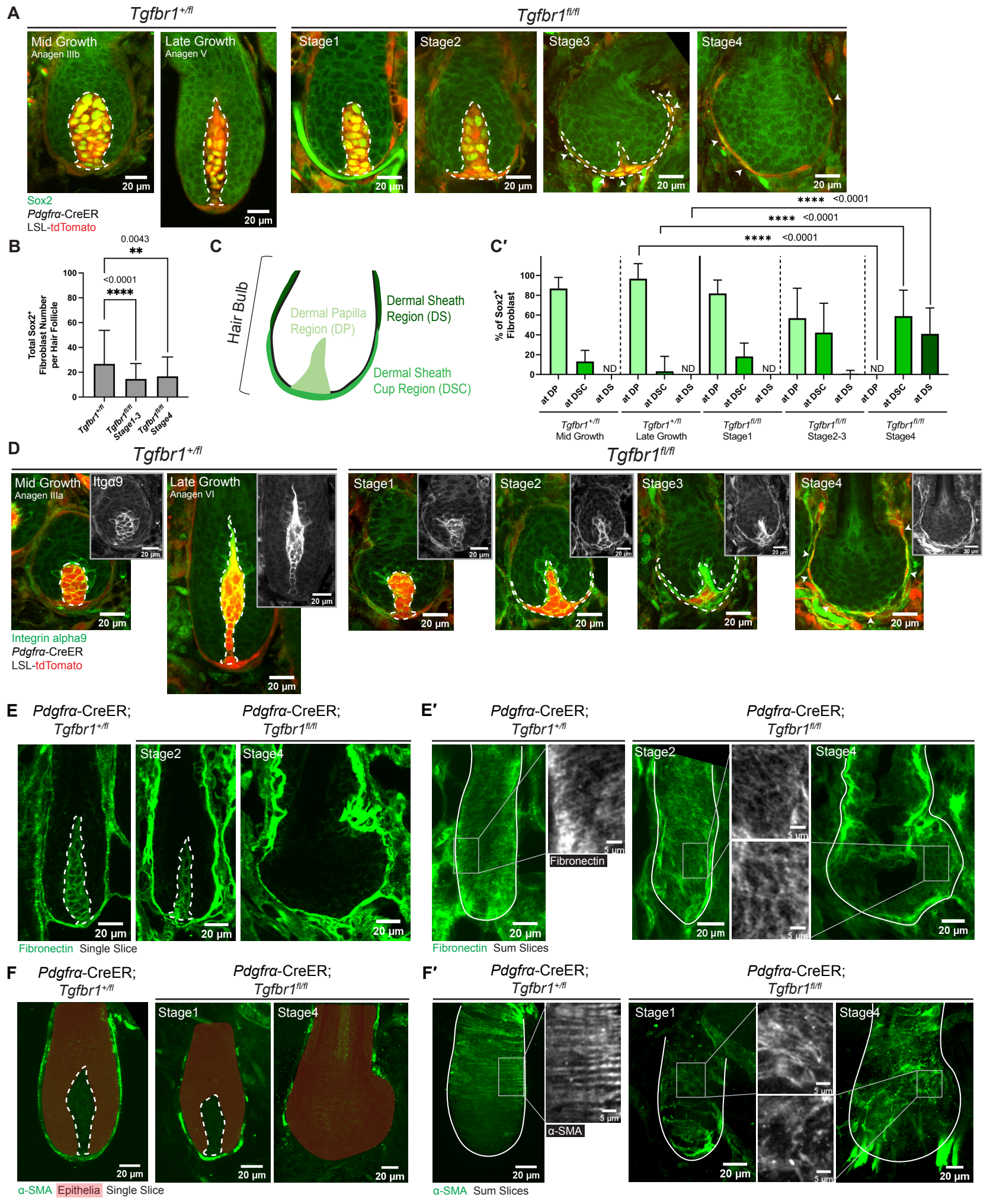

Supplemental Figure 3. Characterization of molecular changes in *Tgfbr1*$^{fl/fl}$ mutant fibroblasts, related to Figure 3

A. Immunostaining for Sox2 (green) in ear skin whole mounts to detect fibroblasts with dermal papilla identity at different stages. Fibroblasts are labeled in red by *Pdgfrα*-CreER; LSL-tdTomato. Dermal papillae are dash-lined. Arrowheads indicate Sox2^{+} fibroblasts in the dermal sheath (cup) regions of *Tgfbr1*$^{fl/fl}$ mutant Stage3 and 4. Images are single optical z slice with scale bar sizes indicated.

B. Total Sox2^{+} fibroblast number per *Tgfbr1*$^{+/fl}$ and *Tgfbr1*$^{fl/fl}$ hair follicle. n=80 mid- and late-growth hair follicles from three *Tgfbr1*$^{+/fl}$ mice, n=110 hair follicles at Stage1-3, and 38 hair follicles at Stage4 from three *Tgfbr1*$^{fl/fl}$ mice. Tukey's multiple comparisons test.

C. Schematic illustrating the regions of dermal papilla, dermal sheath cup, and dermal sheath (in different green colors) around the hair bulb.

C′. Percentage of Sox2^{+} fibroblasts localized at different regions of *Tgfbr1*$^{+/fl}$ and *Tgfbr1*$^{fl/fl}$ hair follicles. ND, not detected. n=36 mid-growth hair follicles, 44 late-growth hair follicles from three *Tgfbr1*$^{+/fl}$ mice, n=42 hair follicles at Stage1, 68 hair follicles at Stage2-3, 38 hair follicles at Stage4 from three *Tgfbr1*$^{fl/fl}$ mice. Tukey's multiple comparisons test.

D. Immunostaining for Integrin alpha9 (Itgα9, green) in ear skin whole mounts to detect fibroblasts with dermal papilla identity at different stages. Fibroblasts are labeled in red by *Pdgfrα*-CreER; LSL-tdTomato. Dermal papillae are dash-lined. Arrowheads indicate Itgα9^{+} cells in the dermal sheath (cup) regions of *Tgfbr1*$^{fl/fl}$ mutant Stage4. Insets show Itgα9 in gray. Images are single optical z slice with scale bar sizes indicated. n=3 *Tgfbr1*$^{+/fl}$ and 3 *Tgfbr1*$^{fl/fl}$ mice.

E. Immunostaining for fibronectin (green) in thick back skin sections to detect the distribution of fibronectin around the hair follicle epithelium at different stages. Dermal papillae are dash-lined. Note that fibronectin remained in the *Tgfbr1*$^{fl/fl}$ mutant dermal papilla at Stage2. Images are single optical z slice with scale bar sizes indicated. n=3 *Tgfbr1*$^{+/fl}$ and 3 *Tgfbr1*$^{fl/fl}$ mice.

E′. Summed optical z slices of immunostained fibronectin (green) to show its organization at the surface of the outlined hair follicles. Insets show cropped regions of fibronectin in gray. Note that fibronectin in *Tgfbr1*$^{fl/fl}$ mutant hair follicles lost the stress fiber-like pattern seen in *Tgfbr1*$^{+/fl}$ control hair follicles. Scale bar sizes are indicated in images. n=3 *Tgfbr1*$^{+/fl}$ and 3 *Tgfbr1*$^{fl/fl}$ mice.

F. Immunostaining for alpha-smooth muscle actin (α-SMA, green) in ear skin whole mounts to detect the distribution of α-SMA around the hair follicle epithelium (red masked) at different stages. Dermal papillae are dash-lined. Images are single optical z slice with scale bar sizes indicated. n=3 *Tgfbr1*$^{+/fl}$ and 3 *Tgfbr1*$^{fl/fl}$ mice.

F′. Summed optical z slices of immunostained α-SMA (green) to show its organization at the surface of outlined hair follicles. Insets show cropped regions of α-SMA in gray. Note that α-SMA in *Tgfbr1*$^{fl/fl}$ mutant hair follicles lost the stress fiber-like pattern seen in *Tgfbr1*$^{+/fl}$ control hair follicles. Scale bar sizes are indicated in images. n=3 *Tgfbr1*$^{+/fl}$ and 3 *Tgfbr1*$^{fl/fl}$ mice.

Supplemental Figure 4. Different hair types and epithelial lineages remain in *Tgfbr1*$^{fl/fl}$ mutant mice but become shorter, related to Figure 4

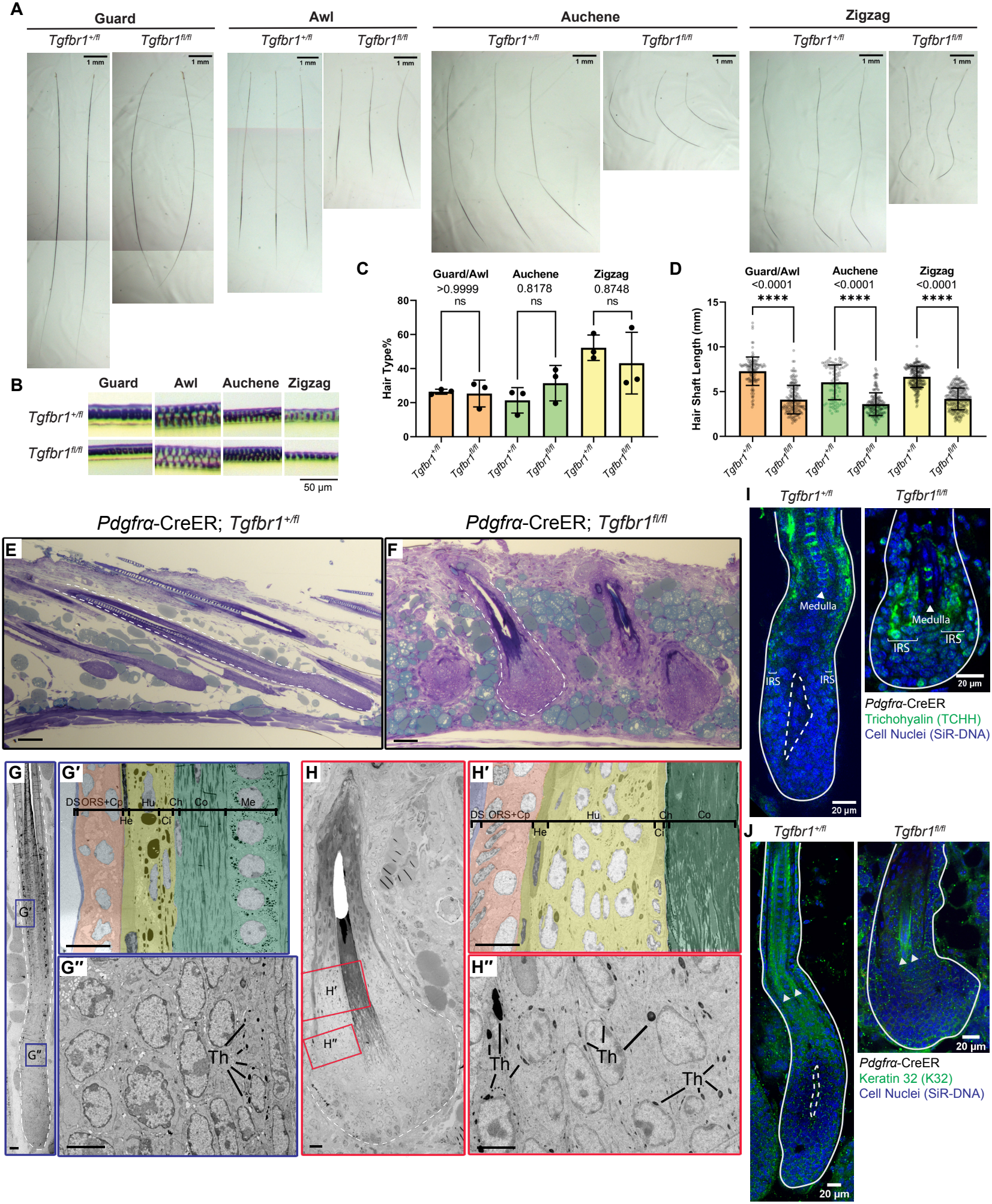

Supplemental Figure 4. Different hair types and epithelial lineages remain in *Tgfbr1*$^{fl/fl}$ mutant mice but become shorter, related to Figure 4

A. Hairs of different types (guard, awl, auchene, zigzag) plucked from *Tgfbr1*$^{+/fl}$ control and *Tgfbr1*$^{fl/fl}$ mutant mice. Mice were shaved at the quiescent stage, and back skin hairs were plucked after an entire first hair cycle. All representative images have scale bar sizes indicated. n=3 *Tgfbr1*$^{+/fl}$ and 3 *Tgfbr1*$^{fl/fl}$ mice.

B. Representative differential interference contrast images to show the medulla lineage (black) present in different types of hair shafts from *Tgfbr1*$^{+/fl}$ control and *Tgfbr1*$^{fl/fl}$ mutant mice. Scale bar=50μm. n=3 *Tgfbr1*$^{+/fl}$ and 3 *Tgfbr1*$^{fl/fl}$ mice.

C. Percentage of different hair types in back skins of *Tgfbr1*$^{+/fl}$ control and *Tgfbr1*$^{fl/fl}$ mutant mice. n=3 *Tgfbr1*$^{+/fl}$ mice (466 plucked hairs), n=3 *Tgfbr1*$^{fl/fl}$ mice (569 plucked hairs). Data are presented as mean ± S.D. and analyzed with Tukey's multiple comparisons test.

D. Hair shaft length of different hair types in *Tgfbr1*$^{+/fl}$ control and *Tgfbr1*$^{fl/fl}$ mutant mice. n=122 guard/awl hairs, 98 auchene hairs, 246 zigzag hairs from three *Tgfbr1*$^{+/fl}$ mice, n=150 guard/awl hairs, 184 auchene hairs, 235 zigzag hairs from three *Tgfbr1*$^{fl/fl}$ mice. Data are presented as mean ± S.D. and analyzed with Tukey's multiple comparisons test.

E-F. Toluidine blue-stained semithin sections from *Tgfbr1*$^{+/fl}$ control and *Tgfbr1*$^{fl/fl}$ mutant mouse back skins. Hair follicles demarcated by dashed white lines are shown in transmission electron micrographs below (Fig.S4G and Fig.S4H). Scale bar in E=100μm, in F=50μm. n=3 *Tgfbr1*$^{+/fl}$ and 3 *Tgfbr1*$^{fl/fl}$ mice.

G-H. Representative transmission electron micrographs of (E) *Tgfbr1*$^{+/fl}$ control and (F) *Tgfbr1*$^{fl/fl}$ mutant hair follicles. Scale bar in G=20μm, in H=10μm.

G′-H′. Upper insets from *Tgfbr1*$^{+/fl}$ control (Fig.S4G) and *Tgfbr1*$^{fl/fl}$ mutant (Fig.S4H) hair follicles. Different layers of the hair follicle are color-coded: green for hair shaft layers (Ch, Co, Me), yellow for inner root sheath layers (He, Hu, Ci), orange for outer root sheath and companion layers (ORS+Cp), and purple for the dermal sheath layer (DS). Different differentiating epithelial lineages are marked in the images: Me, hair shaft medulla; Co, hair shaft cortex; Ch, hair shaft cuticle; Ci, inner root sheath cuticle; Hu, Huxley's layer; He, Henle's layer; Cp, companion layer. Note in *Tgfbr1*$^{fl/fl}$ mutant hair follicles, the medulla (Me) was not consistently detectable, and the inner root sheath Huxley's layer (Hu) expanded into multiple layers. Scale bar in G′ and H′=10μm. n=3 *Tgfbr1*$^{+/fl}$ and 3 *Tgfbr1*$^{fl/fl}$ mice.

G″-H″. Lower insets (just above the matrix) of *Tgfbr1*$^{+/fl}$ control (Fig.S4G) and *Tgfbr1*$^{fl/fl}$ mutant (Fig.S4H) hair follicles. Note the presence of trichohyalin granules (Th) in a single column of inner root sheath progenitor cells in *Tgfbr1*$^{+/fl}$ control (G″) and in multiple columns of cells in *Tgfbr1*$^{fl/fl}$ mutant (H″). Scale bar in G″ and H″=5μm. n=3 *Tgfbr1*$^{+/fl}$ and 3 *Tgfbr1*$^{fl/fl}$ mice.

I. Immunostaining for Trichohyalin (TCHH, green) in thick back skin sections to detect the differentiation of hair shaft medulla and inner root sheath (IRS) lineages. Hair follicles are solid-lined and dermal papilla is dash-lined. Cell nuclei are stained by SiR-DNA in blue. TCHH^{+} inner root sheath lineages are bracketed. TCHH^{+} hair shaft medulla lineages (arrowheads) were detected in the middle of all lineages but were precociously lost in *Tgfbr1*$^{fl/fl}$ mutant. n=3 *Tgfbr1*$^{+/fl}$ and 3 *Tgfbr1*$^{fl/fl}$ mice.

J. Immunostaining for Keratin 32 (K32, green) in thick back skin sections to detect the hair shaft cuticle layer in the hair follicle epithelium. Hair follicles are solid-lined and dermal papilla is dash-lined. Cell nuclei are stained by SiR-DNA in blue. The K32^{+} hair shaft cuticle lineages are marked by arrowheads. n=3 *Tgfbr1*$^{+/fl}$ and 3 *Tgfbr1*$^{fl/fl}$ mice.